Nanoscale Research Letters
a SpringerOpen Journal

NANO IDEA   **Open Access**

Migration of carbon nanotubes from liquid phase to vapor phase in the refrigerant-based nanofluid pool boiling

Hao Peng[1,2], Guoliang Ding[1*], Haitao Hu[1]

Abstract

The migration characteristics of carbon nanotubes from liquid phase to vapor phase in the refrigerant-based nanofluid pool boiling were investigated experimentally. Four types of carbon nanotubes with the outside diameters from 15 to 80 nm and the lengths from 1.5 to 10 μm were used in the experiments. The refrigerants include R113, R141b and *n*-pentane. The oil concentration is from 0 to 10 wt.%, the heat flux is from 10 to 100 kW·m^{-2}, and the initial liquid-level height is from 1.3 to 3.4 cm. The experimental results indicate that the migration ratio of carbon nanotube increases with the increase of the outside diameter or the length of carbon nanotube. For the fixed type of carbon nanotube, the migration ratio decreases with the increase of the oil concentration or the heat flux, and increases with the increase of the initial liquid-level height. The migration ratio of carbon nanotube increases with the decrease of dynamic viscosity of refrigerant or the increase of liquid phase density of refrigerant. A model for predicting the migration ratio of carbon nanotubes in the refrigerant-based nanofluid pool boiling is proposed, and the predictions agree with 92% of the experimental data within a deviation of ±20%.

Introduction

Nowadays, the researchers show great interest in the possible application of refrigerant-based nanofluids (i.e., the mixtures of nanopowders and conventional pure refrigerants) for improving the performance of refrigeration systems. The researches showed that the refrigerant-based nanofluids have higher thermal conductivity than those of conventional pure refrigerants [1], the addition of nanoparticles enhances the solubility of mineral oil in HFC refrigerant [2], and the addition of nanoparticles can save energy consumption of air-conditioner and refrigerator [3,4]. Comparing with the spherical metal or metal oxide nanoparticles used in these researches, carbon nanotubes (CNTs) have one or two orders of magnitude higher in thermal conductivity, and CNTs can significantly enhance the thermal conductivity of base fluid [5-8] as well as the convective heat transfer coefficient of base fluid [9], so CNTs have great potential for improving the performance of refrigeration systems. For applying CNTs in refrigeration systems, the phase-change heat transfer characteristics of refrigerant-CNT nanofluid and the cycle behavior of CNTs in refrigeration systems should be known. The migration of CNTs from liquid phase to vapor phase in the pool boiling process of refrigerant-CNT nanofluid determines the distribution of CNTs concentration in the liquid phase and vapor phase, and then has significant effect on the phase-change heat transfer characteristics of refrigerant-CNT nanofluid as well as the cycle behavior of CNTs. Therefore, in order to evaluate the phase-change heat transfer characteristics of refrigerant-CNT nanofluid and the cycle behavior of CNTs, the migration of CNTs in the pool boiling process of refrigerant-CNT nanofluid should be researched.

The migration of CNTs from liquid phase to vapor phase in the refrigerant-based nanofluid pool boiling can be divided to the following four physical processes: (1) the departure of bubble from the heating surface, (2) the movement of bubble and CNTs in the liquid phase, (3) the capture of CNTs by bubble, and (4) the escape of CNTs from the liquid-vapor interface. From the above analysis, it can be seen that the interaction between CNTs and bubble is the key factor causing the migration of CNTs from liquid phase to vapor phase. The existing flotation theory can accurately describe the

* Correspondence: glding@sjtu.edu.cn
[1]Institute of Refrigeration and Cryogenics, Shanghai Jiaotong University, 800 Dongchuan Road, Shanghai 200240, China
Full list of author information is available at the end of the article

SpringerOpen

interaction between particles and bubbles. However, they can not directly used to predict the migration of CNTs from liquid phase to vapor phase during pool boiling because they are aimed at the conditions without phase change. The present investigation is beneficial to reveal the mass transfer mechanism of nano-scale solid powders from liquid phase to vapor phase during the phase-change process of fluid, and provides the theoretical basis for evaluating the phase-change heat transfer characteristics of refrigerant-CNT nanofluid and the cycle behavior of CNTs.

Until now, there is no published research on the migration characteristics of CNTs in the pool boiling of refrigerant-based nanofluid. The migration characteristics of nanopowders are mentioned only by the paper of Ding et al. [10], and are focused on one type of spherical nanoparticle (CuO). In the paper, the authors found that the migrated mass of CuO nanoparticles in the pool boiling increases with the increase of the original mass of nanoparticles or the original mass of refrigerant. As the structure and the thermophysical properties of CNTs are different from those of spherical nanoparticles, the migration characteristics of CNTs in the pool boiling of refrigerant-based nanofluid may be different from those of spherical nanoparticles, and should be investigated.

The existing researches on the pool boiling heat transfer characteristics of nanofluids containing CNTs can be divided into three categories as follows: (1) Pool boiling heat transfer of water-CNTs nanofluids. The experimental results showed that CNTs can enhance the pool boiling heat transfer of water [11-13] or deteriorate the pool boiling heat transfer of water [14], and the influence of CNTs on the pool boiling is related to CNTs concentration [13]. (2) Pool boiling heat transfer of pure refrigerant-CNTs nanofluids. The experiments by Park and Jung [11,15] showed that CNTs can enhance the pool boiling heat transfer of pure refrigerants (R22, R123, and R134a), and the enhancement is related to the heat flux. (3) Pool boiling heat transfer of refrigerant-oil mixtures with CNTs. Experiments by Peng et al. [16] showed that CNTs can enhance the pool boiling heat transfer of refrigerant-oil mixtures, and the enhancement increases with the decrease of CNTs' outside diameter or CNTs' nanolubricant mass fraction, while increases with the increase of CNTs' length or CNTs' mass fraction in the CNTs' nanolubricant. From the above researches, it can be seen that the CNTs physical dimension (i.e., the outside diameter and the length of CNTs), refrigerant type, CNTs concentration, oil concentration, and heat flux have influences on the pool boiling heat transfer of refrigerant-based nanofluid. Therefore, the influences of the above factors on the migration characteristics of CNTs need be concerned.

In addition, the initial liquid-level height affects the pool boiling heat transfer, so the influence of initial liquid-level height on the migration characteristics of CNTs also needs be concerned.

The objective of this paper is to experimentally investigate the influences of CNTs physical dimension, refrigerant type, oil concentration, heat flux, and initial liquid-level height on the migration characteristics of CNTs in the refrigerant-based nanofluid pool boiling at different original CNTs concentrations, and to propose a model for predicting the migration ratio of CNTs in the refrigerant-based nanofluid pool boiling.

Experiments

Test conditions and experimental objects

Test conditions are divided into five categories, as tabulated in Table 1.

The objective of category 1 is to investigate the influences of CNTs physical dimension on the migration characteristics of CNTs. Four types of CNTs with different physical dimensions (numbered as CNT#1, CNT#2, CNT#3, and CNT#4) produced by the chemical vapor deposition method are used in these test conditions. The physical dimensions of these four types of CNTs are shown in Table 2 and the TEM (transmission electron microscope) photographs of the CNTs are shown in Figure 1. In these test conditions, the other influence factors including the refrigerant type, oil concentration, heat flux and initial liquid-level height are fixed.

The objective of category 2 is to investigate the influences of refrigerant type on the migration characteristics of CNTs. Three types of refrigerants including R113, R141b, and *n*-pentane are used in these test conditions, belonging to CFC refrigerant, HCFC refrigerant, and alkane refrigerant, respectively. The reasons for choosing these three types of refrigerants are as follows: (1) R113, R141b and *n*-pentane are in liquid state at room temperature and atmospheric pressure while the widely used refrigerants (e.g., R410A) are in vapor state, so it is much easier to prepare refrigerant-based nanofluids based on R113, R141b, or *n*-pentane. (2) These three types of refrigerants have different chemical and thermophysical properties including molecular mass, density, dynamic viscosity, etc. The properties of these three refrigerants are given in Table 3. In these test conditions, the other influence factors including the CNTs physical dimension, oil concentration, heat flux and initial liquid-level height are fixed.

The objective of category 3 is to investigate the influences of oil concentration on the migration characteristics of CNTs. The lubricating oil RB68EP is used in the experiments. RB68EP is an ester oil with a density of 0.964 g·cm^{-3} at 15°C and kinematic viscosities of 66.79 and 8.23 mm^2·s^{-1} at 40°C and 100°C, respectively, as

Table 1 Test conditions

Objective of investigation	CNTs type	Refrigerant type	Oil concentration x_o (wt.%)	Heat flux q (kWm^{-2})	Initial liquid-level height L (cm)	Original CNTs concentration ϕ_n (vol.%)
Influence of CNTs physical dimension on migration	CNT#1, CNT#2, CNT#3, CNT#4	R113	0	50	2.0	0.56, 1.11, 1.65, 2.19, 2.72, 3.25, 3.77
Influence of refrigerant type on migration	CNT#2	R113, R141b, *n*-pentane	0	50	2.0	0.56, 1.11, 1.65, 2.19, 2.72, 3.25, 3.77
Influence of oil concentration on migration	CNT#2	R113	1, 5, 10	50	2.0	0.56, 1.11, 1.65, 2.19, 2.72, 3.25, 3.77
Influence of heat flux on migration	CNT#2	R113	0	10, 20, 50, 100	2.0	0.56, 1.11, 1.65, 2.19, 2.72, 3.25, 3.77
Influence of initial liquid-level height on migration	CNT#2	R113	0	50	1.3, 2.0 2.7, 3.4	0.56, 1.11, 1.65, 2.19, 2.72, 3.25, 3.77

reported by the manufacturer. The oil concentration is from 0 to 10 wt.%, covering the oil concentration in the actual refrigeration system. In these test conditions, the other influence factors including the CNTs physical dimension, refrigerant type, heat flux and initial liquid-level height are fixed.

The objective of category 4 is to investigate the influences of heat flux on the migration characteristics of CNTs. The heat flux is from 10 to 100 kW·m^{-2}, covering the heat flux in the actual refrigeration system. In these test conditions, the other influence factors including the CNTs physical dimension, refrigerant type, oil concentration and initial liquid-level height are fixed.

The objective of category 5 is to investigate the influences of initial liquid-level height on the migration characteristics of CNTs. The initial liquid-level height is from 1.3 to 3.4 cm. In these test conditions, the other influence factors including the CNTs physical dimension, refrigerant type, oil concentration, and heat flux are fixed.

Experimental apparatus

The experimental apparatus used for testing the migration characteristics of CNTs in the refrigerant-based nanofluid pool boiling mainly consists of a pool boiling device, a capture cover and a digital electronic balance, as schematically shown in Figure 2. The pool boiling device mainly consists of a boiling vessel and an electric heating membrane. The boiling vessel is a cylindrical glass container with the inside diameter of 50 mm and the height of 95 mm. The vessel is insulated with glass

fibers to reduce heat loss to the surroundings. The electric heating membrane is connected with the direct-current voltage power supply. The ampere meter with the calibrated precision of 0.5% is used for reading electric current supplied to the heating surface, and a data acquisition system with the calibrated precision of 0.002% is used to measure the voltage across the heating surface. The heat flux through the heating surface is controlled by adjusting the heating power of the plate heater, and is calculated by the measured electric current, voltage, and heating surface area. The uncertainty of heat flux is estimated to be smaller than 1.2%. The capture cover is used to collect the CNTs spouted to the environment. The measurement range of the digital electronic balance is from 10.0 mg to 210.0000 g, and the maximum error is 0.1 mg. All the experiments are performed at atmospheric pressure (101.3 kPa) by venting the boiling vessel to ambient.
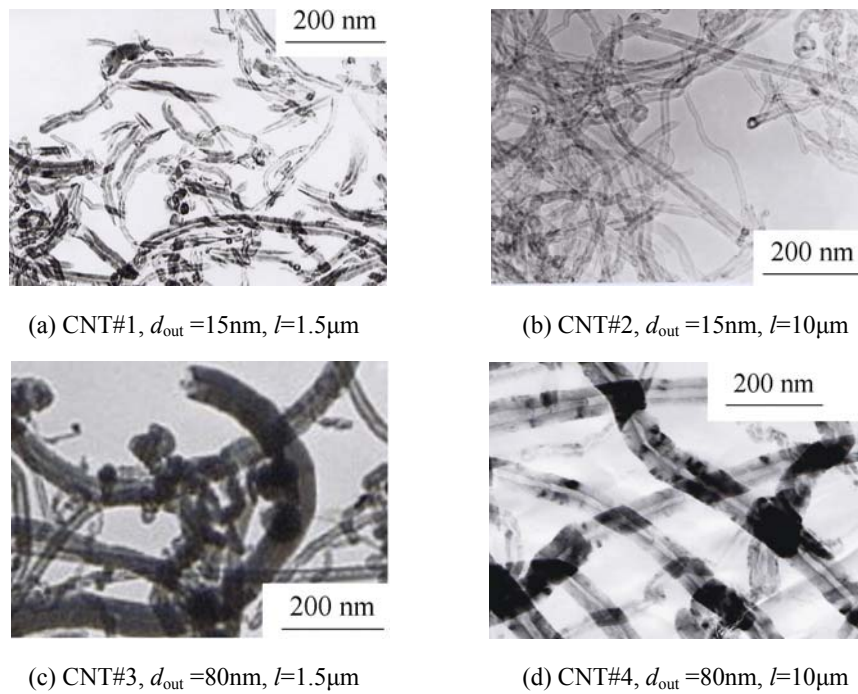
Experimental method

The objective of the measurements is to get the migrated mass of CNTs from liquid phase to vapor phase in the refrigerant-based nanofluid pool boiling. Ding et al. [10] have proposed the weighing method to obtain the migrated mass of spherical nanoparticles, and this method is also used in the present study to get the migrated mass of CNTs.

The experimental procedure for the refrigerant-based nanofluid without oil consists of the following steps: (1) adding CNTs with the original mass of m_{n0} to the

Table 2 Physical dimensions of CNTs

Property	Mean outside diameter (d_{out})	Mean inside diameter (d_{in})	Mean length (l)	Aspect ratio (l/d_{out})
CNT#1	15 nm	10 nm	1.5 μm	100
CNT#2	15 nm	10 nm	10 μm	666.7
CNT#3	80 nm	18 nm	1.5 μm	18.8
CNT#4	80 nm	18 nm	10 μm	125

(a) CNT#1, d_{out} =15nm, l=1.5μm

(b) CNT#2, d_{out} =15nm, l=10μm

(c) CNT#3, d_{out} =80nm, l=1.5μm

(d) CNT#4, d_{out} =80nm, l=10μm

Figure 1 TEM photographs of CNTs. **(a)** CNT#1; **(b)** CNT#2; **(c)** CNT#3; **(d)** CNT#4.

boiling vessel; (2) weighing the total mass of the boiling vessel and the CNTs, m_1; (3) adding refrigerant with the original mass of m_{r0} to the boiling vessel; (4) opening the direct-current voltage power supply and heating the refrigerant-based nanofluid to be boiling; (5) adjusting the voltage to control the heat flux; (6) weighing the total mass of the boiling vessel and the CNTs, m_2, when the refrigerant is entirely evaporated (the signal for the entire evaporation is that the mass of mixture does not change for 12 h); (7) calculating the migrated mass of CNTs with the equation $\Delta m_n = m_1 - m_2$.

The experimental procedure for the refrigerant-based nanofluid with oil consists of the following steps: (1) adding CNTs with the original mass of m_{n0} and oil with the mass of m_o to the boiling vessel; (2) weighing the total mass of the boiling vessel, the CNTs and oil, m_3;

(3) adding refrigerant with the original mass of m_{r0} to the boiling vessel; (4) opening the direct-current voltage power supply and heating the refrigerant-based nanofluid with lubricating oil to be boiling; (5) adjusting the voltage to control the heat flux; (6) weighing the total mass of the boiling vessel, the CNTs and oil, m_4, when the refrigerant is entirely evaporated (the signal for the entire evaporation is that the mass of mixture does not change for 12 h); (7) calculating the migrated mass of CNTs with the equation $\Delta m_n = m_3 - m_4$.

Data reduction and uncertainty

In order to quantitatively evaluate the migration degree of CNTs, the migration ratio of CNTs, ζ, is defined by Eq. 1:

$$\zeta = \Delta m_n / m_{n0} \qquad (1)$$

Table 3 Properties of refrigerants in the experiments

Property	R113	R141b	*n*-Pentane
Chemical formula	Cl2FC-CClF2	CH3CCl2F	C5H12
Molecular mass (g/mol)	187.37	116.95	72.15
Normal boiling point (°C)	47.6	32.05	36.1
Liquid-phase density (kg·m^{-3})	1508	1220	606
Vapor-phase density(kg·m^{-3})	7.4	4.8	3.2
Liquid-phase dynamic viscosity (Pa·s)	5×10^{-4}	3.78×10^{-4}	1.91×10^{-4}
Liquid-phase isobaric specific heat (J·kg^{-1}·K^{-1})	940	1,165	2,441
Surface tension (N·m^{-1})	0.0147	0.0173	0.0138
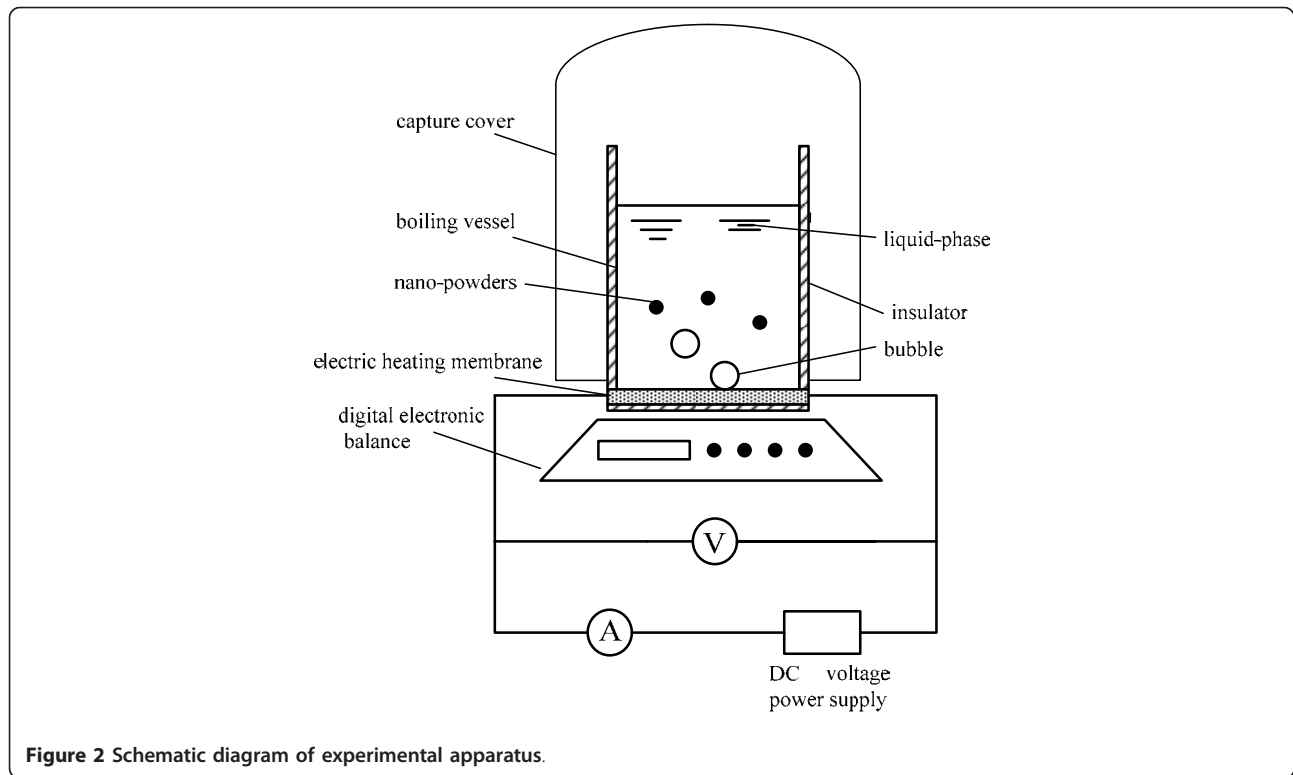
Figure 2 Schematic diagram of experimental apparatus.

where, Δm_n is the migrated mass of CNTs, and m_{n0} is the original mass of CNTs.

The original CNTs concentration is defined as the original volume fraction of CNTs in the liquid phase (liquid refrigerant or liquid refrigerant-oil mixture), presented as Eq. 2:

$$\varphi_n = \frac{m_{n0}/\rho_n}{m_{n0}/\rho_n + m_{r0}/\rho_{r,L} + m_o/\rho_o} \qquad (2)$$

where, m_{r0}, m_o are the original mass of refrigerant and the mass of oil, respectively; ρ_n, $\rho_{r,L}$, ρ_o are the density of CNTs, liquid-phase refrigerant and oil, respectively.

The oil concentration is defined as the original mass fraction of oil in the liquid refrigerant-oil mixture, presented as Eq. 3:

$$x_o = \frac{m_o}{m_{r0} + m_o} \qquad (3)$$

The relative uncertainty of migration ratio of CNTs is calculated as:

$$\frac{\delta\zeta}{\zeta} = \sqrt{\left(\frac{1}{\Delta m_n}\right)^2 \delta\Delta m_n{}^2 + \left(\frac{1}{m_{n0}}\right)^2 \delta m_{n0}{}^2} \qquad (4)$$

Determined by the accuracy of the digital electronic balance, the maximum uncertainties of the measured migrated mass of CNTs ($\delta\Delta m_n$) and original mass of

CNTs (δm_0) are 0.2 mg and 0.1 mg, respectively. The maximum relative uncertainty of migration ratio of CNTs is obtained at the condition of the smallest migrated mass of CNTs and the migrated mass of CNTs, and calculated to be 2.5%.

Tests under several conditions were repeated for three times, and it shows that the differences among the three testing results under each condition are less than 3%. Therefore, the experimental results are reproducible.

Experimental results and analysis

Influence of CNTs physical dimension on the migration of CNTs

Figure 3 shows the migration ratio (ζ) of CNTs as a function of original CNTs concentration (ϕ_n) for CNTs with different physical dimensions. The values of ζ under these test conditions are in the range of 5.1% to approximately 27.8%. For fixed CNTs physical dimension, ζ decreases with the increase of ϕ_n. For example, ζ for CNT#1 decreases by 15.8% with the increase of ϕ_n from 0.56 to 3.77 vol.%.

From Figure 3 it can be seen that the migration ratio (ζ) of CNTs increases with the increase of the outside diameter of CNTs (d_{out}) when the length of CNTs (l) is fixed. For example, at the condition of l = 1.5 μm, the value of ζ increases by maximally 286.4% with the increase of d_{out} from 15 to 80 nm. It also can be seen from Figure 3 that the migration ratio (ζ) of CNTs
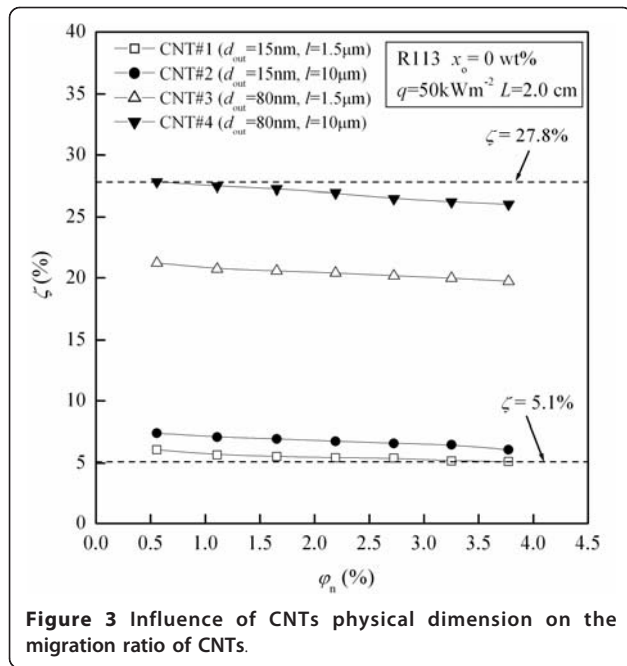
Figure 3 Influence of CNTs physical dimension on the migration ratio of CNTs.
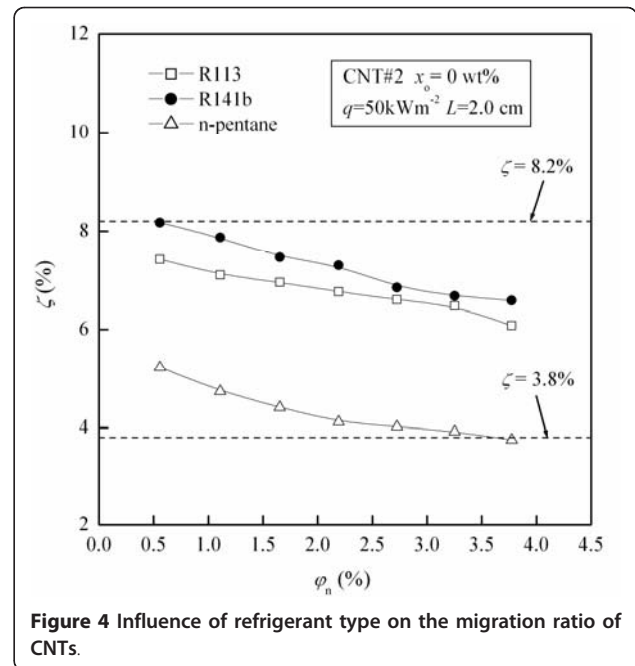
Figure 4 Influence of refrigerant type on the migration ratio of CNTs.

increases with the increase of the length of CNTs (l) when the outside diameter of CNTs (d_{out}) is fixed. For example, at the condition of d_{out} = 15 nm, the value of ζ increases by maximally 25.7% with the increase of l from 1.5 to 10 μm. The possible reasons for the above phenomenon are as follows: The capture of CNTs by the bubbles generated in the pool boiling leads to the migration of CNTs. Brownian diffusion, interception, gravity settling and inertial impaction are four mechanisms for the capture of particles by bubbles [17]. As the CNTs do not exhibit Brownian motion due to their high aspect ratio [18,19], the capture efficiency of CNTs by bubbles can be considered as the sum of the capture efficiencies caused by interception, gravity settling, and inertial impaction. Each of the above three captured efficiencies increases with Stokes diameter of CNTs. The increase of the outside diameter or the length of CNTs causes the increase of Stokes diameter of CNTs [20], thus the captured efficiency of CNTs by bubbles increases, which leads to the migration ratio (ζ) of CNTs increasing with increase of the outside diameter or the length of CNTs.

Influence of refrigerant type on the migration of CNTs
Figure 4 shows the migration ratio (ζ) of CNTs as a function of original CNTs concentration (ϕ_n) for different types of refrigerants. The values of ζ under these test conditions are in the range of 3.8% to approximately 8.2%. For fixed refrigerant type, ζ decreases with the increase of ϕ_n. For example, ζ for R141b decreases by 19.5% with the increase of ϕ_n from 0.56 to 3.77 vol.%.

From Figure 4 it can be seen that the migration ratio (ζ) of CNTs are in the order of R141b > R113 >*n*-pentane, the value of ζ in the R141b-based nanofluid is by maximally 10.7% larger than that in the R113-based nanofluid, and is by maximally 77.4% larger than that in *n*-pentane-based nanofluid. The possible reasons for the above phenomenon are as follows: (1) The dynamic viscosity values for these three refrigerants are in the order of R113 (5×10^{-4} Pa·s) > R141b (3.78×10^{-4} Pa·s) >*n*-pentane (1.91×10^{-4} Pa·s). The larger dynamic viscosity causes the smaller capture efficiencies caused by gravity settling and inertial impaction, which leads to the smaller migration ratio of CNTs. (2) The liquid-phase density values of for these three refrigerants are in the order of R113 (1,508 kg·m^{-3}) > R141b (1,220 kg·m^{-3}) >*n*-pentane (606 kg·m^{-3}). The larger liquid-phase density means the larger mass of liquid-phase refrigerant at fixed liquid-level height, thus the amount of bubbles generated in the pool boiling is larger, which leads to the larger migration ratio of CNTs. The influence of refrigerant type on the migration ratio of CNTs is determined by the conjunct role of the above two aspects, and follows the order of R141b > R113 >*n*-pentane. It can be concluded that the migration ratio of carbon nanotube increases with the decrease of dynamic viscosity of refrigerant or the increase of liquid-phase density of refrigerant.

Influence of oil concentration on the migration of CNTs
Figure 5 shows the migration ratio (ζ) of CNTs as a function of original CNTs concentration (ϕ_n) for

Figure 5 Influence of oil concentration on the migration ratio of CNTs.

**Figure 6 Influence of heat flux on the migration ratio of CNTs**.
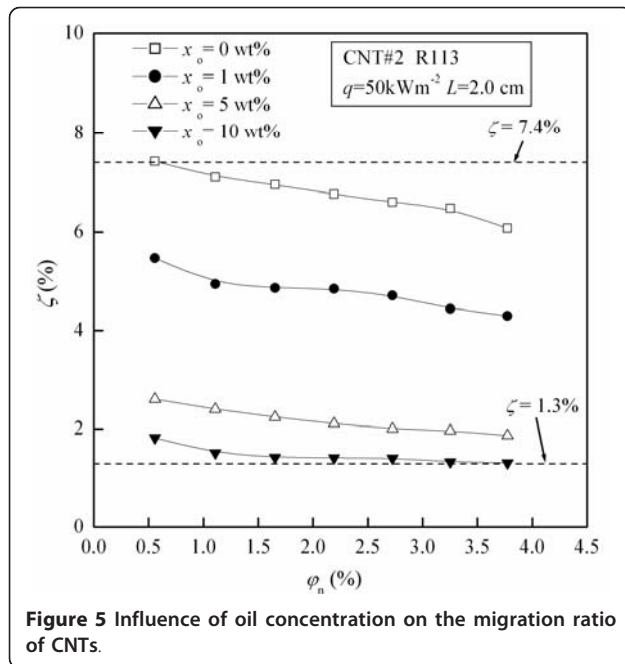
different oil concentrations (x_o). The values of ζ under these test conditions are in the range of 1.3% to approximately 7.4%. For fixed x_o, ζ decreases with the increase of ϕ_n. For example, at the condition of $x_o = 5$ wt.%, ζ decreases by 28.2% with the increase of ϕ_n from 0.56 to 3.77 vol.%.

From Figure 5 it can be seen that the migration ratio (ζ) of CNTs decreases by maximally 70.7% with the increase of oil concentration (x_o) from 1 to 10 wt.%. The possible reasons are as follows: (1) The dynamic viscosity and surface tension of lubricating oil RB68EP are larger than those of pure refrigerant, causing the dynamic viscosity and surface tension of liquid-phase refrigerant-oil mixture increase with the increase of x_o. (2) The increase of dynamic viscosity of liquid-phase refrigerant-oil mixture results in the decrease of capture efficiencies caused by gravity settling and inertial impaction, which leads to ζ decreasing with the increase of x_o. (3) The increase of surface tension of liquid-phase refrigerant-oil mixture causes the increase of bubble departure diameter in the pool boiling, thus the capture efficiencies caused by interception, gravity settling, and inertial impaction decrease, which leads to ζ decreasing with the increase of x_o.

Influence of heat flux on the migration of CNTs
Figure 6 shows the migration ratio (ζ) of CNTs as a function of original CNTs concentration (ϕ_n) for different heat fluxes (q). The values of ζ under these test conditions are in the range of 5.5% to approximately 9.2%. For fixed q, ζ decreases with the increase of ϕ_n. For
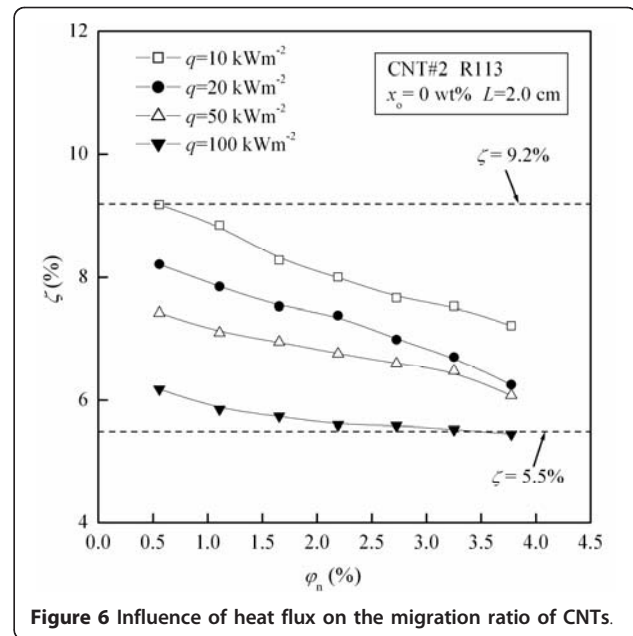
example, at the condition of $q = 10$ kWm^{-2}, ζ decreases by 21.5% with the increase of ϕ_n from 0.56 to 3.77 vol.%.

From Figure 6 it can be seen that the migration ratio (ζ) of CNTs decreases by maximally 33.9% with the increase of heat flux (q) from 10 to 100 kWm^{-2}. The possible reasons are as follows: (1) The increase of heat flux causes the increase of the velocity of departure bubble [21], thus the velocity of rising bubble increases. (2) The increase of velocity of rising bubble results in the decrease of capture efficiency caused by gravity settling, which leads to the decrease of ζ. (3) The increase of velocity of rising bubble results in the increase of capture efficiency caused by inertial impaction, which leads to the increase of ζ. (4) The increase of velocity of rising bubble results in the decrease of the bubble rising time in the liquid phase, causing the decrease of the amount of CNTs captured by bubbles, which leads to the decrease of ζ. The conjunct role of the above aspects leads to the migration ratio of CNTs (ζ) decreasing with the increase of heat flux.

Influence of liquid-level height on the migration of CNTs
Figure 7 shows the migration ratio (ζ) of CNTs as a function of original CNTs concentration (ϕ_n) for different initial liquid-level heights (L). The values of ζ under these test conditions are in the range of 3.2% to approximately 19.8%. For fixed L, ζ decreases with the increase of ϕ_n. For example, at the condition of $L = 2.7$ cm, ζ decreases by 16.5% with the increase of ϕ_n from 0.56 to 3.77 vol.%.

From Figure 7 it can be seen that the migration ratio (ζ) of CNTs increases by maximally 446.9% with the
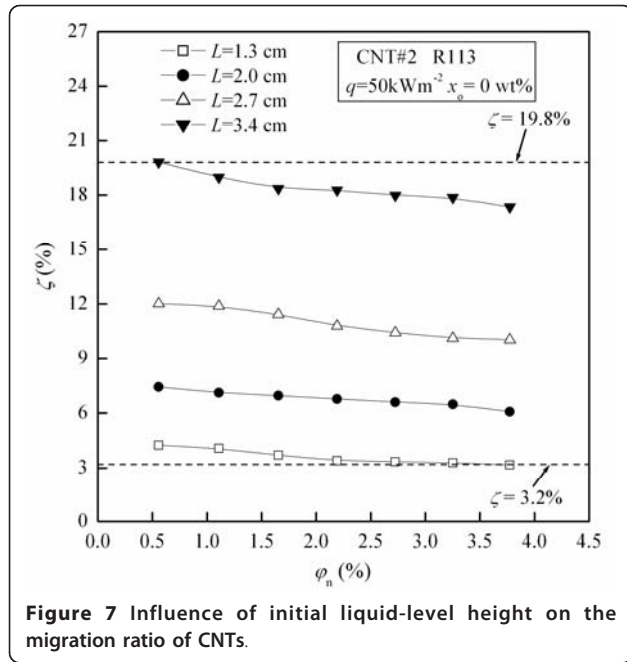
Figure 7 Influence of initial liquid-level height on the migration ratio of CNTs.

increase of initial liquid-level height (L) from 1.3 to 3.4 cm. The possible reasons are as follows: (1) The increase of initial liquid-level height causes the increase of the bubble rising time in the liquid phase, thus the amount of CNTs captured by bubbles, which leads to ζ increasing with the increase of liquid-level height. (2) The increase of initial liquid-level height causes the increase of CNTs escape probability on the liquid-vapor interface, which leads to ζ increasing with the increase of liquid-level height.

Prediction of migration ratio of CNTs in the refrigerant-based nanofluid pool boiling

As there is no published literature on the model for predicting the migration ratio of CNTs in the refrigerant-based nanofluid pool boiling, the development of a new model is needed. The CNTs physical dimension, refrigerant type, oil concentration, heat flux, and initial liquid-level height are five important factors influencing the migration of CNTs, and should be reflected in the new model.

From the beginning of the pool boiling t_0 to the moment of t, the migration ratio of CNTs can be expressed as:

$$\zeta_{t_0 - t} = 1 - \frac{m_{n,t}}{m_{n0}} \tag{5}$$

where, $m_{n,t}$ is the mass of CNTs in the liquid phase at the moment of t; m_{n0} is the original mass of CNTs.

According to the principle of mass conservation, the mass of CNTs in the liquid phase changed with time can be expressed as:

$$\frac{dm_{n,t}}{dt} = -K n_b m_{n,t} \tag{6}$$

where, K is the migration coefficient of CNTs (i.e., the migration proportion of CNTs caused by single bubble); n_b is the number of generated bubbles per unit time. From Eq. 6, the following equation can be obtained.

$$m_{n,t} = m_{n0} \cdot \exp(-K n_b t) \tag{7}$$

Combing Eqs. 5 and 7, $\zeta_{t_0 - t}$ can be calculated as:

$$\zeta_{t_0 - t} = 1 - \exp(-K n_b t) \tag{8}$$

Therefore, from the beginning to the end of pool boiling, the migration ratio of CNTs is:

$$\zeta = 1 - \exp(-K N_b) \tag{9}$$

In Eq. 9, N_b is the total number of generated bubbles from the beginning to the end of pool boiling.

1. The calculation of K

The migration of CNTs can be considered as the capture of CNTs by bubbles combining the escape of CNTs from the liquid-vapor interface. In order to describe the capture process of CNTs by bubbles, the capture efficiencies of CNTs caused by interception, gravity settling and inertial impaction should be included in K. In order to describe the escape process of CNTs from the liquid-vapor interface, the escape probability of CNTs should be included in K. The original CNTs concentration has influences on the bubble diameter and bubble rising velocity during the pool boiling process of refrigerant-based nanofluid, and then has influence on the migration of CNTs. Therefore, the CNTs concentration impact factor should also be included in K. The expression of K is as follows:

$$K = (\alpha_I + \alpha_G + \alpha_{IN}) \beta \gamma \tag{10}$$

where, α_I, α_G, and α_{IN} are the capture efficiencies of CNTs caused by interception, gravity settling, and inertial impaction, respectively; β is the escape probability of CNTs; γ is the CNTs concentration impact factor. α_I, α_G, α_{IN}, β, and γ are expressed as Eqs. 11 to 15, respectively.

$$\alpha_I = a_1 \cdot \left(\frac{d_S}{d_b}\right)^{b_1} \tag{11}$$

$$\alpha_I = a_2 \cdot \left(\frac{u_n}{u_b}\right)^{b_2} = a_2 \cdot \left(\frac{g(\rho_n - \rho_L) d_S^2}{18 \mu_L u_b}\right)^{b_2} \tag{12}$$

$$\alpha_{\text{IN}} = a_3 \cdot \text{St}^{b_3} = a_3 \cdot \left(\frac{d_{\text{S}}^2 \rho_{\text{n}} u_{\text{b}}}{18 d_{\text{b}} \mu_{\text{L}}} \right)^{b_3} \tag{13}$$

$$\beta = \left(\frac{D}{H - L/2} \right)^{b_4} \tag{14}$$

$$\gamma = a_4 \cdot \varphi_{\text{n}}^{b_5} \tag{15}$$

In Eqs. 11 to 15, D and H are the bottom diameter and height of boiling vessel, respectively; ρ_{L}, ρ_{b}, ρ_{n} are the density of liquid refrigerant-oil mixture, bubble and CNT, respectively; μ_{L} is the dynamic viscosity of liquid refrigerant-oil mixture; d_{s} is the Stokes diameter; d_{b} is the diameter of bubble; u_{b} is the bubble rising velocity. The calculation of ρ_{L} and m_{L} are presented in -Table 4.

d_{s} can be calculated by Eq. 16 [20]:

$$d_{\text{S}} = d_{\text{out}} \sqrt{\text{Ln}(2l/d_{\text{out}})} \tag{16}$$

d_{b} can be calculated by Cole-Rohsenow correlation [22], as shown in Eq. 17:

$$d_{\text{b}} = 4.65 \times 10^{-4} \left(\frac{\rho_{\text{L}} C_{p,\text{L}} T_{\text{sat}}}{\rho_{\text{b}} h_{\text{fg}}} \right)^{\frac{5}{4}} \left(\frac{\sigma}{g(\rho_{\text{L}} - \rho_{\text{b}})} \right)^{\frac{1}{2}} \tag{17}$$

u_{b} can be calculated by Malenkov correlation [21], as shown in Eq. 18:

$$u_{\text{b}} = \left[\frac{d_{\text{b}} g (\rho_{\text{L}} - \rho_{\text{b}})}{2(\rho_{\text{L}} + \rho_{\text{b}})} + \frac{2\sigma g}{d_{\text{b}}(\rho_{\text{L}} + \rho_{\text{b}})} \right]^{1/2} + \frac{q}{h_{\text{fg}} \rho_{\text{b}}} \tag{18}$$

In Eqs. 17 and 18, $C_{p,\text{L}}$ is the isobaric specific heat of liquid refrigerant-oil mixture; σ is the surface tension of refrigerant-oil mixture; T_{sat} is the saturation temperature; h_{fg} is the latent heat of vaporization. The calculation of $C_{p,\text{L}}$ and σ are presented in -Table 4.

2. The calculation of N_{b}

As the original mass of refrigerant is equal to the total mass of generated bubbles from the beginning to the end of pool boiling, N_{b} can be calculated by Eq. 19.

$$N_{\text{b}} = \frac{3D^2 H (1 - x_{\text{o}}) \rho_{\text{L}}}{2 \rho_{\text{b}} d_{\text{b}}^3} \tag{19}$$

The nine coefficients of a_1, a_2, a_3, a_4, b_1, b_2, b_3, b_4, and b_5 in Eqs. 11 to 15 are fitted based on total 105 experimental data in this study. By nonlinear programming solution method, the nine coefficients of a_1, a_2, a_3, a_4, b_1, b_2, b_3, b_4, and b_5 can be determined as 0.1, 6.3 × 10^{-6}, 1,995.3, 66.9, 2.34, 0.4, 2.26, 8.78, and -0.09, respectively. Therefore, the model for predicting the migration ratio of CNTs in the refrigerant-based nanofluid pool boiling is expressed Eq. 20.

$$\zeta = 1 - \exp \left\{ -66.9 \left[0.1 \left(\frac{d_{\text{S}}}{d_{\text{b}}} \right)^{2.34} + 6.3 \times 10^{-6} \left(\frac{g(\rho_{\text{n}} - \rho_{\text{L}}) d_{\text{S}}^2}{18 \mu_{\text{L}} u_{\text{b}}} \right)^{0.4} \right. \right.$$
$$\left. \left. + 1995.3 \left(\frac{d_{\text{S}}^2 \rho_{\text{n}} u_{\text{b}}}{18 d_{\text{b}} \mu_{\text{L}}} \right)^{2.26} \right] \left(\frac{D}{H - L/2} \right)^{8.78} \frac{3D^2 H (1 - x_{\text{o}}) \rho_{\text{L}}}{2 \rho_{\text{b}} d_{\text{b}}^3} \varphi_{\text{n}}^{-0.09} \right\} \tag{20}$$

Figure 8a to e shows the comparison between the predicted values of the model with the experimental data for different CNTs physical dimensions, refrigerant types, oil concentrations, heat fluxes, and liquid-level heights, respectively. It can be seen from Figure 8a to e that the migration ratio of CNTs predicted by the model and the experimental data have the same tendency changing with the CNTs physical dimension, refrigerant type, oil concentration, heat flux, or initial liquid-level height. The predicted values of the model agree with 92% of the experimental data of migration ratio of CNTs within a deviation of ± 20%, and the mean deviation is 9.96%.

Conclusions

Migration characteristics of CNTs from liquid phase to vapor phase in the pool boiling process of refrigerant-based nanofluid are investigated experimentally, and some conclusions are obtained.

1. The migration ratio of CNTs increases with the increase of the outside diameter of CNTs or the length of CNTs.

2. The migration ratio of carbon nanotube increases with the decrease of dynamic viscosity of refrigerant or the increase of liquid-phase density of refrigerant. Under the present experimental conditions, the migration ratio of CNTs in the R141b-based nanofluid is by maximally 10.7% larger than that in the R113-based nanofluid, and is by maximally 77.4% larger than that in *n*-pentane-based nanofluid.

Table 4 Calculation of the properties of liquid refrigerant-oil mixture

Property	Model for calculating property	Author
Specific heat ($J \cdot kg^{-1} \cdot K^{-1}$)	$C_{p,\text{L}} = (1 - x_{\text{o}}) C_{p,\text{r}} + x_{\text{o}} C_{p,\text{o}}$ (A1)	Jensen and Jackman [23]
Viscosity (Pa·s)	$\mu_{\text{L}} = e^{(x_{\text{o}} \ln \mu_{\text{o}} + (1 - x_{\text{o}}) \ln \mu_{\text{r}})}$ (A2)	Kedzierski and Kaul [24]
Surface tension ($N \cdot m^{-1}$)	$\sigma = \sigma_{\text{r}} + (\sigma_{\text{o}} - \sigma_{\text{r}}) x_{\text{o}}^{0.5}$ (A3)	Jensen and Jackman [23]
Density ($kg \cdot m^{-3}$)	$\rho_{\text{L}} = \left(\frac{x_{\text{o}}}{\rho_{\text{o}}} + \frac{1 - x_{\text{o}}}{\rho_{\text{r}}} \right)^{-1}$ (A8)	
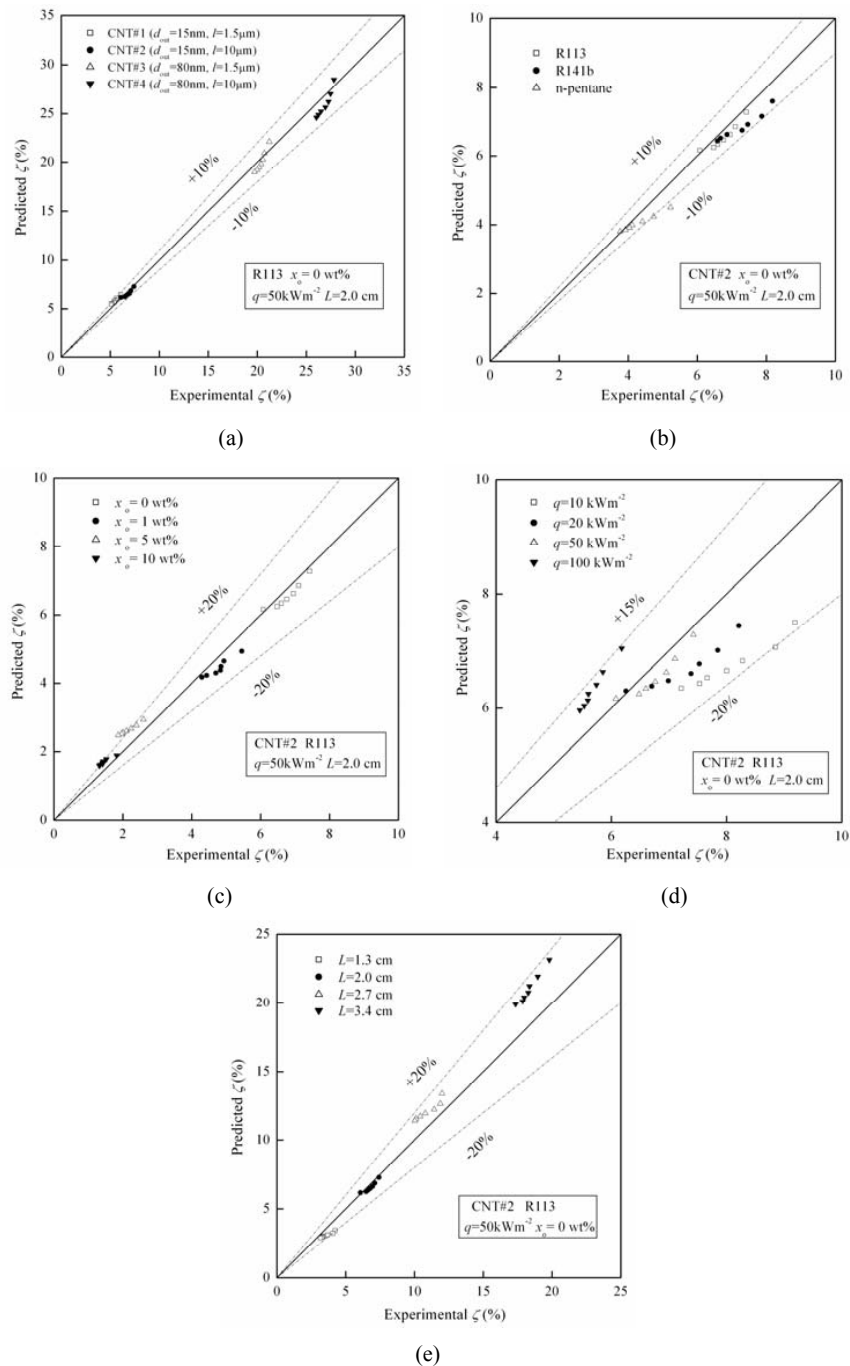
Figure 8 Comparison between the predicted migration ratios of the model with the experimental data. **(a)** for different CNTs physical dimensions; **(b)** for different refrigerant types; **(c)** for different oilconcentrations; **(d)** for different heat fluxes; **(e)** for different initial liquid-level heights.

3. The migration ratio of CNTs decreases with the increase of oil concentration. Under the present experimental conditions, the migration ratio decreases by maximally 70.7% with the increase of oil concentration from 1 to 10 wt.%.

4. The migration ratio of CNTs decreases with the increase of heat flux. Under the present experimental conditions, the migration ratio decreases by maximally 33.9% with the increase of heat flux from 10 to 100 kWm^{-2}.

5. The migration ratio of CNTs increases with the increase of initial liquid-level height. Under the present experimental conditions, the migration ratio increases by maximally 446.9% with the increase of initial liquid-level height from 1.3 to 3.4 cm.

6. A model for predicting the migration ratio of CNTs in the refrigerant-based nanofluid pool boiling is proposed, and the predicted values of the model can agree with 92% of the experimental data of migration ratio of CNTs within a deviation of ± 20%.

Author details
[1]Institute of Refrigeration and Cryogenics, Shanghai Jiaotong University, 800 Dongchuan Road, Shanghai 200240, China [2]Key Laboratory of Microgravity (National Microgravity Laboratory)/CAS; Institute of Mechanics, Chinese Academy of Sciences (CAS), 15 Beisihuan Xilu, Beijing 100190, China

Authors' contributions
HP carried out the experimental study and model development. GD participated in the model development and design of the experiments. HH participated in the experimental study. All authors read and approved the final manuscript.

Competing interests
The authors declare that they have no competing interests.

References
1. Jiang WT, Ding GL, Peng H, Gao YF, Wang KJ: **Experimental and model research on thermal conductivity of nanorefrigerant.** *HVAC&R Research* 2009, **15**(3):651-669.
2. Wang RX, Hao B, Xie GZ: **A refrigerating system using HFC134a and mineral lubricant appended with n-TiO$_2$(R) as working fluids.** *Proceedings of the 4th International Symposium on HAVC, Tsinghua University Press, Beijing, China* 2003, 888-892.
3. Wang KJ, Shiromoto K, Mizogami T: **Experiment study on the effect of nano-scale particle on the condensation process.** *Proceedings of the 22nd International Congress of Refrigeration, Beijing, China, Paper No* 2007, B1-1005.
4. Bi SS, Shi L, Zhang LL: **Application of nanoparticles in domestic refrigerators.** *Applied Thermal Engineering* 2008, **28**:1834-1843.
5. Choi US, Zhang ZG, Yu W, Lockwood FE, Grulke EA: **Anomalous thermal conductivity enhancement in nanotube suspensions.** *Applied Physics Letters* 2001, **79**:2252-2254.
6. Xie HQ, Lee H, Youn W, Choi M: **Nanofluids containing multiwalled carbon nanotubes and their enhanced thermal conductivities.** *Journal of Applied Physics* 2003, **94**:4967-4971.
7. Assael MJ, Chen CF, Metaxa I, Wakeham WA: **Thermal conductivity of suspensions of carbon nanotubes in water.** *International Journal of Thermophysics* 2004, **25**:971-985.
8. Hwang YJ, Ahn YC, Shin HS, Lee CG, Kim GT, Park HS, Lee JK: **Investigation on characteristics of thermal conductivity enhancement of nanofluids.** *Current Applied Physics* 2006, **6**:1068-1071.
9. Ding YL, Alias H, Wen DS, Williams RA: **Heat transfer of aqueous suspensions of carbon nanotubes (CNT nanofluids).** *International Journal of Heat and Mass Transfer* 2006, **49**(1-2):240-250.
10. Ding GL, Peng H, Jiang WT, Gao YF: **The migration characteristics of nanoparticles in the pool boiling process of nanorefrigerant and nanorefrigerant-oil mixture.** *International Journal of Refrigeration* 2009, **32**(1):114-123.
11. Park KJ, Jung DS: **Enhancement of nucleate boiling heat transfer using carbon nanotubes.** *International Journal of Heat and Mass Transfer* 2007, **50**:4499-4502.
12. Kathiravan R, Kumar R, Gupta A, Chandra R, Jain PK: **Pool boiling characteristics of carbon nanotube based nanofluids over a horizontal tube.** *Journal of Thermal Science and Engineering Applications* 2009, **1**(2):022001..
13. Liu ZH, Yang XF, Xiong JG: **Boiling characteristics of carbon nanotube suspensions under sub-atmospheric pressures.** *International Journal of Thermal Sciences* 2010, **49**(7):1156-1164.
14. Park KJ, Jung DS, Shim SE: **Nucleate boiling heat transfer in aqueous solutions with carbon nanotubes up to critical heat fluxes.** *International Journal of Multiphase Flow* 2009, **35**:525-532.
15. Park KJ, Jung DS: **Boiling heat transfer enhancement with carbon nanotubes for refrigerants used in building air-conditioning.** *Energy and Buildings* 2007, **39**(9):1061-1064.
16. Peng H, Ding GL, Hu HT, Jiang WT: **Influence of carbon nanotubes on nucleate pool boiling heat transfer characteristics of refrigerant-oil mixture.** *International Journal of Thermal Sciences* 2010, **49**(12):2428-2438.
17. Edzwald JK, Malley JP, Yu C: **A conceptual model for dissolved air flotation in water treatment.** *Water Supply* 1990, **8**:141-150.
18. Prasher R, Phelan PE, Bhattachary P: **Effect of aggregation kinetics on the thermal Conductivity of nanoscale colloidal solutions (nanofluid).** *Nano Letters* 2006, **6**(7):1529-1534.
19. Xie HQ, Chen LF: **Adjustable thermal conductivity in carbon nanotube nanofluids.** *Physics Letters A* 2009, **373**:1861-1864.
20. Henn AR: **Calculation of the stokes and aerodynamic equivalent diameters of a short reinforcing fiber.** *Particle & Particle Systems Characterization* 1996, **13**(4):249-253.
21. Malenkov IG: **Detachment frequency as a function of size for vapor bubbles.** *Journal of Engineering Physics and Thermophysics* 1971, **20**(6):704-708.
22. Cole R, Rosenhow W: **Correlation of bubble departure diameters for boiling of saturated liquids.** *Chem Eng Prog Symp Ser* 1969, **65**(92):211-213.
23. Jensen MK, Jackman DL: **Prediction of nucleate pool boiling heat transfer coefficients of refrigerant-oil mixtures.** *Journal of Heat Transfer* 1984, **106**:184-190.
24. Kedzierski MA, Kaul MP: **Horizontal nucleate flow boiling heat transfer coefficient measurements and visual observations for R12, R134a, and R134a/ester lubricant mixtures.** *Proceedings of the 6th International Symposium on Transport Phenomena in Thermal Engineering* 1993, **1**:111-116.